Bull Volcanol (2015) 77: 90
DOI 10.1007/s00445-015-0974-3

RESEARCH ARTICLE

Disruption of tephra fall deposits caused by lava flows during basaltic eruptions

R. J. Brown[1] · **T. Thordarson**[2] · **S. Self**[3] · **S. Blake**[3]

Received: 12 December 2014 / Accepted: 10 September 2015 / Published online: 18 September 2015

Abstract Observations in the USA, Iceland and Tenerife, Canary Islands reveal how processes occurring during basaltic eruptions can result in complex physical and stratigraphic relationships between lava and proximal tephra fall deposits around vents. Observations illustrate how basaltic lavas can disrupt, dissect (spatially and temporally) and alter sheet-form fall deposits. Complexity arises through synchronous and alternating effusive and explosive activity that results in intercalated lavas and tephra deposits. Tephra deposits can become disrupted into mounds and ridges by lateral and vertical displacement caused by movement (including inflation) of underlying pāhoehoe lavas and clastogenic lavas. Mounds of tephra can be rafted away over distances of 100 s to 1,000 s m from proximal pyroclastic constructs on top of lava flows. Draping of irregular topography by fall deposits and subsequent partial burial of topographic depressions by later lavas can result in apparent complexity of tephra layers. These processes, deduced from field relationships, have resulted in considerable stratigraphic complexity in the studied proximal regions where fallout was synchronous or alternated with inflation of subjacent lava sheets. These mechanisms may lead to diachronous contact relationships between fall deposits and lava flows. Such complexities may remain cryptic due to textural and geochemical quasi-homogeneity within sequences of interbedded basaltic fall deposits and lavas. The net effect of these processes may be to reduce the usefulness of data collected from proximal fall deposits for reconstructing basaltic eruption dynamics.

Keywords Pāhoehoe · Lava · Tephra fall deposit · Basaltic eruption

Editorial responsibility: M.R. Patrick

✉ R. J. Brown
Richard.brown3@durham.ac.uk

[1] Department of Earth Sciences, Durham University, Science Labs, Durham DH1 3LE, UK

[2] Faculty of Earth Sciences, University of Iceland, Vestbær, Reykjavik, Iceland

[3] Volcano Dynamics Group, Department of Environmental, Earth and Ecosystems, Open University, Walton Hall, Milton Keynes MK7 6AA, UK

Introduction

Basaltic eruptions commonly emit both lava and pyroclasts. Often, these products are produced simultaneously or alternate between the two (e.g. 1959–1960 eruption of Kīlauea volcano, Hawai i, Richter et al. 1970; 1991 eruption of Hekla, Iceland, Gudmundsson et al. 1992; see Pioli et al. 2009). Coarse molten pyroclasts can coalesce at the base of a fire fountain and flow away as lava (Parcheta et al. 2012) at the same time as fine pyroclasts are thermally lofted into a drifting ash plume (e.g. Lopez et al. 2014) or ballistically carried far enough to fall as solids. Basaltic eruptions can be protracted, lasting for years to decades (e.g. Miocene Roza Lava flow, Columbia River Basalt Group, Thordarson and Self 1998; Pu u Ō ō-Kūpaianaha, Kīlauea, Hawai i, Heliker et al. 2003; Jorullo, Mexico, Rowland et al. 2009), and can be characterised by many eruptive events spread out through time and space along a fissure or amongst several vents (e.g. Fedotov et al. 1980; Carracedo et al. 1992; Thordarson and Self 1993). A corollary of multivent eruptions is that products from different vents can interact and overlap with each other to produce complex stratigraphic and physical relationships (1783–1785 Laki eruption, Iceland; Thordarson and Self 1993; Brown et al. 2014). As a result, proximal areas around vents are dynamic, constantly changing physical environments during eruptions (Holm 1987;

Valentine et al. 2006; Riggs and Duffield 2008). Disentangling eruptive sequences in proximal regions by study of the emitted products can be demanding and, for Quaternary-to-recent eruptions, is often hampered by the burial of early products beneath later products (e.g. proximal pyroclastic deposits of the Laki eruption, Thordarson and Self 1993). In the case of long-lived, large-volume flood basalt eruptions, lava can cover hundreds to thousands of square kilometres in all directions away from a vent, and in some cases, almost all pyroclastic material can become buried during the course of the later stages of an eruption (e.g. Brown et al. 2014).

Understanding the nature of these interactions can help in the piecing together of eruption histories because deposits hold a wealth of information that can be used to infer eruption dynamics (e.g. column heights, mass fluxes, durations, steadiness; Carey and Sparks 1986; Wilson and Walker 1987; Pyle 1989; Parfitt and Wilson 1999; Houghton et al. 2006) and to elucidate landscape evolution in proximal regions. However, in order to extract useful information, individual layers need to be confidently traced away from the vent to construct isopachs and isopleths and to establish stratigraphic relationships. This is not always easy. Several common characteristics of basaltic eruptions can reduce the confidence with which fall deposits can be traced away from source. Firstly, many erupted basaltic magmas are chemically monotonous and even large-volume eruptions can exhibit minimal change in geochemistry through time (e.g. Roza and Sand Hollow lava flow fields, Columbia River Basalt Group; Martin 1989; Vye-Brown et al. 2013; 1783–1875 Laki eruption, Iceland, Sigmarsson et al. 1991; Passmore et al. 2012). Secondly, sustained, steady phases of eruptions produce pyroclastic deposits that can be massive and texturally homogeneous and that lack traceable layers.

In this paper, our purpose is to outline some of the ways in which proximal pyroclastic fall deposits can become disrupted by lavas during basaltic eruptions. We then describe some of the complex physical and stratigraphic relationships that can result from these processes. We use examples from historic eruptions and from the geologic record (Table 1). We discuss the implications of these processes for understanding landscape evolution, eruption dynamics and emplacement mechanisms in proximal environments during basaltic eruptions. We illustrate that these processes may inhibit the collection of accurate isopleth and isopach data in proximal areas through the generation of allochthonous tephra deposits and through the modification of a deposit's original thickness.

Field data on disrupted basaltic fall deposits

Roza Member, Columbia River Basalt Group, USA

The Roza Member in the Columbia River Basalt Group (CRBG) is a 1,300-km^3 flood basalt flow field covering ~40,300 km^2 of the states of Washington and Oregon (Martin 1989; Thordarson and Self 1998; Fig. 1). It comprises four major lava flows and at most localities it is formed of one to three stacked sheet lobes, which together can reach over 70 m thick. The Roza dike vent system can be traced for >180 km from NE Oregon into SE Washington (Swanson et al. 1975; Brown et al. 2014). Proximal tephra fall deposits are exposed around fissure segments at the northern end of the Roza vent system (Swanson et al. 1975; Fig. 1). Ten fissure vent localities have been recognised north of the Snake River (Brown et al. 2014), over an along-strike distance of 30 km. These pyroclastic rocks outcrop over minimum areas of 0.5–2 km^2 and are inferred to have originally formed cones, ramparts and sheets comprised of scoria, densely welded spatter, spatter-fed lava and spongy pāhoehoe (Swanson et al. 1975; Brown et al. 2014). Large spatter bombs constrain the location of the vents to within several hundred metres and record fallout under lava fountains. Cone-forming pyroclastic deposits can exceed 50 m thick, and all vents were substantially buried by later-emplaced Roza lava in the same prolonged eruption (Brown et al. 2014).

Tephra deposits are particularly well-exposed in natural and man-made sections around the town of Winona, Washington State (Fig. 2; e.g. Thordarson and Self 1996; Brown et al. 2014). Here, the base of the Roza Member is not exposed and the lowest Roza product is a poorly exposed lava flow with the surface characteristics of rubbly pāhoehoe (e.g. Keszthelyi et al. 2004; Guilbaud et al. 2005; Duraiswami et al. 2008). It is overlain by pyroclastic deposits, the source of which is inferred to be a fissure vent that is exposed in a 2D east–west-oriented railway cut 500 m to the west (Fig. 2). The position of the vent is constrained by two, discontinuously exposed, opposing accumulations of densely welded spatter and scoria that built up on either side of a fissure (Fig. 2; Brown et al. 2014). The spatter deposits generally dip at low angles away from the fissure and thin from >20 to <2 m over a horizontal distance >500 m. In proximal regions, dense welding means that the outlines of constituent spatter bombs are not visible. Instead, the rock appears glassy with thin wispy fiamme inferred to be remnant vesicular interiors of bombs (Thordarson and Self 1996, 1998; Brown et al. 2014). With distance, the welding intensity decreases and the outlines of spatter and scoria bombs are apparent. The welding intensity appears to decrease upwards, although these deposits are inaccessible. The vent is filled with a later-emplaced lava sheet lobe, and the whole sequence is capped by an even later 20 m thick Roza sheet lobe (Fig. 2).

At distances of 800–1,500 m from the fissure, tephra deposits comprise non-welded, well-sorted ($\sigma\varphi$=~1), massive to weakly horizontally bedded lapilli (Thordarson and Self 1998). The fall deposits exhibit unusual geometries and stratigraphic relationships with interbedded, thin, highly vesicular and rubbly pāhoehoe lavas (Fig. 3a, b). At the base of this

Table 1 Localities of key examples of the features described in the text

Feature	Location	Country	Grid reference
Dissected tephra fall deposits	Winona	Washington, USA	46° 56′ 36.17″ N, 117° 47′ 37.31″ W
	Little Sheep Creek	Oregon, USA	45° 20′ 8.15″N, 117° 4′ 48.61″ W
	Chinyero	Tenerife, Spain	28° 17′ 39.76″ N, 16° 45′ 16.53″ W
	Laki (Hnúta)	Iceland	64° 00′ 21.39″ N, 18° 22′ 28.71″ W
	Laki (Varmárdalur)	Iceland	64° 02′ 24.11″ N, 18° 16′ 47.65″ W
	Hekla	Iceland	63° 59′ 18.09″ N, 19° 38′ 12.38″ W
Intercalated lava and tephra	Winona	Washington, USA	46° 56′ 35.11″ N, 117° 48′ 22.05″ W
	Lancaster Road	Washington, USA	46° 57′ 28.31″ N, 117° 48′ 30.66″ W
Rafted tephra deposits	Mason Draw	Washington, USA	46° 57′ 33.59″ N, 117° 51′ 9.35″ W
	Winona	Washington, USA	46° 56′ 15.49″ N, 117° 49′ 33.62″ W
	Palouse River	Washington, USA	46° 55′ 10.77″ N, 117° 51′ 7.37″ W
	Chinyero	Tenerife, Spain	28° 17′ 28.66″ N, 16° 45′ 25.75″ W

succession is a pāhoehoe lava flow whose upper, highly vesicular crust is rubbly and consists of jumbled slabs and blocks that range in size from <0.1 to 1.5 m (Fig. 3a). The slabs and blocks have vesicularities up to 50 vol%, and some exhibit ropy fluidal exteriors and sheared vesicles. Some of the larger slabs are steeply to vertically oriented (Fig. 3b). The upper

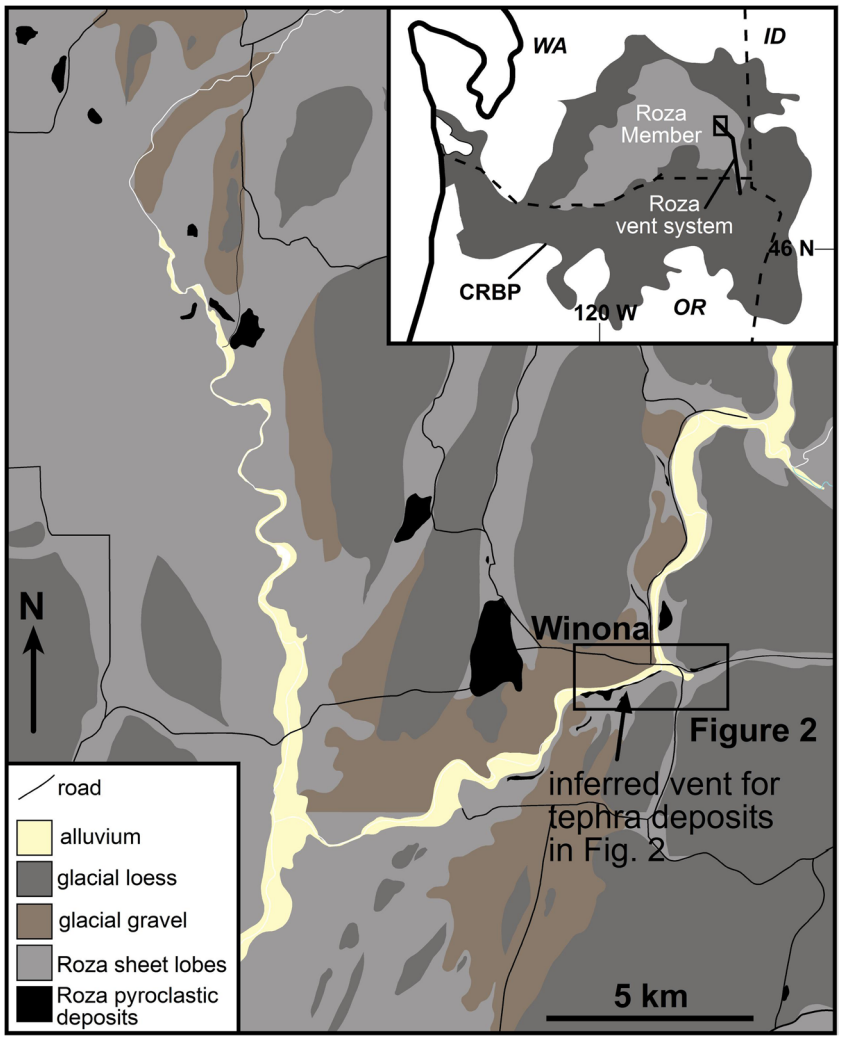

Fig. 1 Geological sketch map of pyroclastic deposits at the northern end of the Roza vent system, CRBG (modified from Brown et al. 2014)

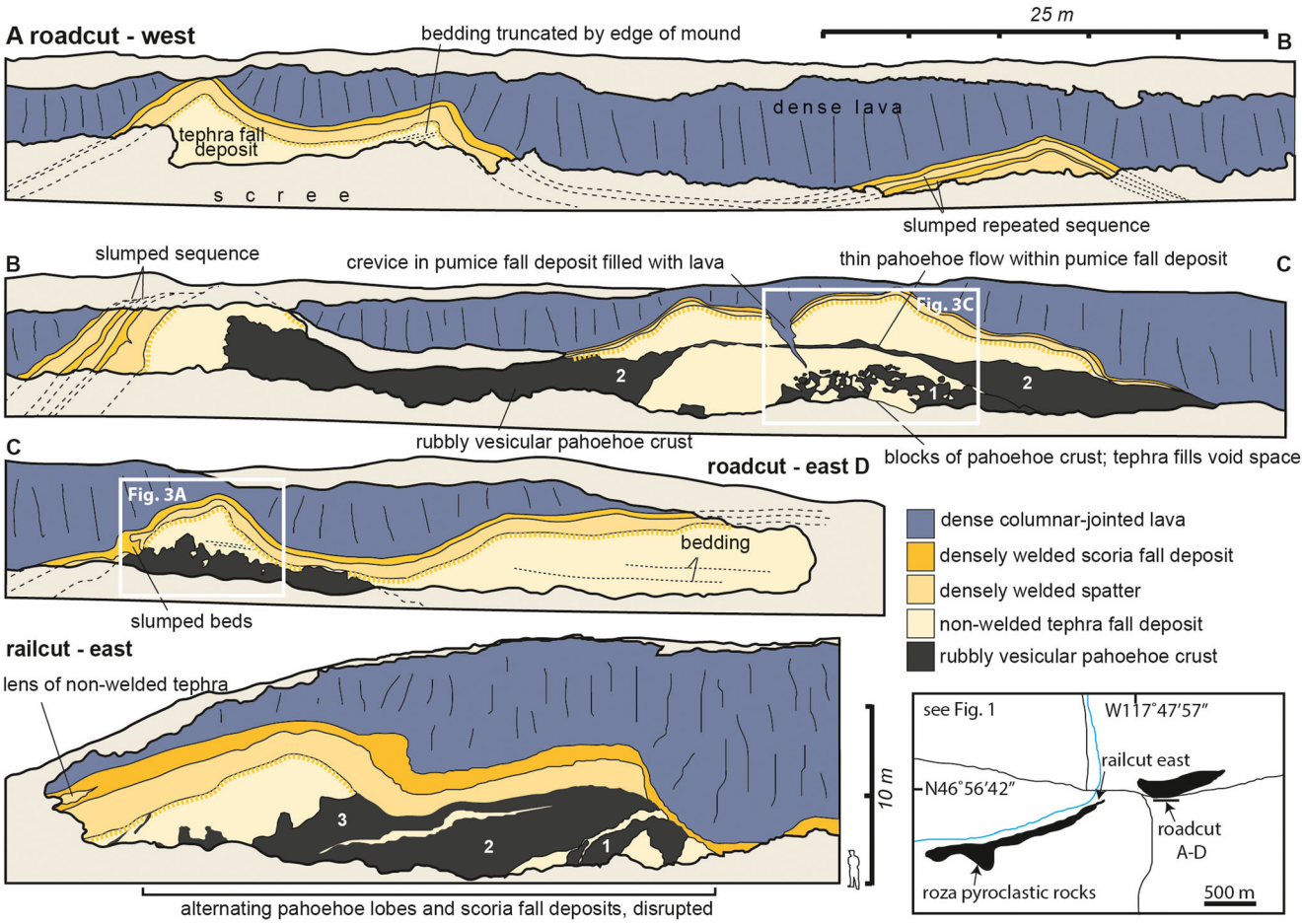

Fig. 2 Interpretations of man-made cuts through the Roza Member at Winona (Table 1), illustrating how a tephra fall deposit has been dissected into a number of mounds and the complex stratigraphic relationships between pyroclastic rocks and lavas. The mounds have been draped by later welded spatter and tephra fall deposits. The inferred vent for the pyroclastic deposits lies ~500 m towards the east of the illustrated rail cut. For location, see Fig. 1. *White rectangles* show locations of Fig. 3a, c. Scale applies to all parts

surface of this lava flow exhibits relief of 1–5 m and is the lowest unit exposed in the area; only the topographic highs along its upper surface are exposed at the base of artificial cuttings. Overlying this is a broad, smooth-surfaced mound of well-sorted, poorly consolidated to unconsolidated, angular, medium lapilli tephra (up to 2 cm in diameter; Fig. 3c, d). This mound is up to 4 m high and 20 m wide. The lapilli tephra fills the void space between the blocks and slabs of the underlying vesicular lava crust. Draping this mound of scoria is a second pāhoehoe lava flow that has been disrupted into decimetre-sized, joint-bounded, angular and vesicular blocks (Fig. 2). The lava is >3 m thick in the topographic depressions on either side of the mound and thins to <30 cm thick over the top. Where the mound pinches out to the east the second lava lies on top of the first. This second lava appears to be of limited extent (Figs. 2 and 3). Overlying the second lava is a series of tephra mounds exposed over a lateral distance of ~200 m (Fig. 2). They are similar in texture, grain size and composition to the lower tephra mound. The tephra clasts are moderately clay altered, but some pockets of pristine tephra are present within the mounds: the density of the lapilli clasts ranges from 400 to 1,200 kg/m^3, which equates to vesicularity values of 55–85 % using a magma density of 2,700 kg/m^3 (Brown et al. 2014). Each mound is up to 5 m thick, up to 30 m wide, and they are spaced ~25–40 m apart (centre-to-centre; Table 2). They are typically massive, although at some outcrops, bedding is poorly defined by several slightly finer-grained horizons each several centimetres thick. These mounds have flat-topped, peaked or convex morphologies (Table 2) with outer slopes of 20–60°. Some mounds are linked to each other, but others are seemingly detached from neighbouring mounds, at least in 2D (Fig. 2). In some of the mounds, sub-horizontal bedding is present. The mounds all occur along the same stratigraphic horizon and feature sub-horizontal bedding and are therefore taken to be part of the same fall deposit (Brown et al. 2014).

The lava flows underlying the mounds are poorly exposed and vary considerably. At some locations, they are composed of lobes several metres thick and up to 50 m wide. However, at the eastern end of the rail cut at Winona, three thin vesicular

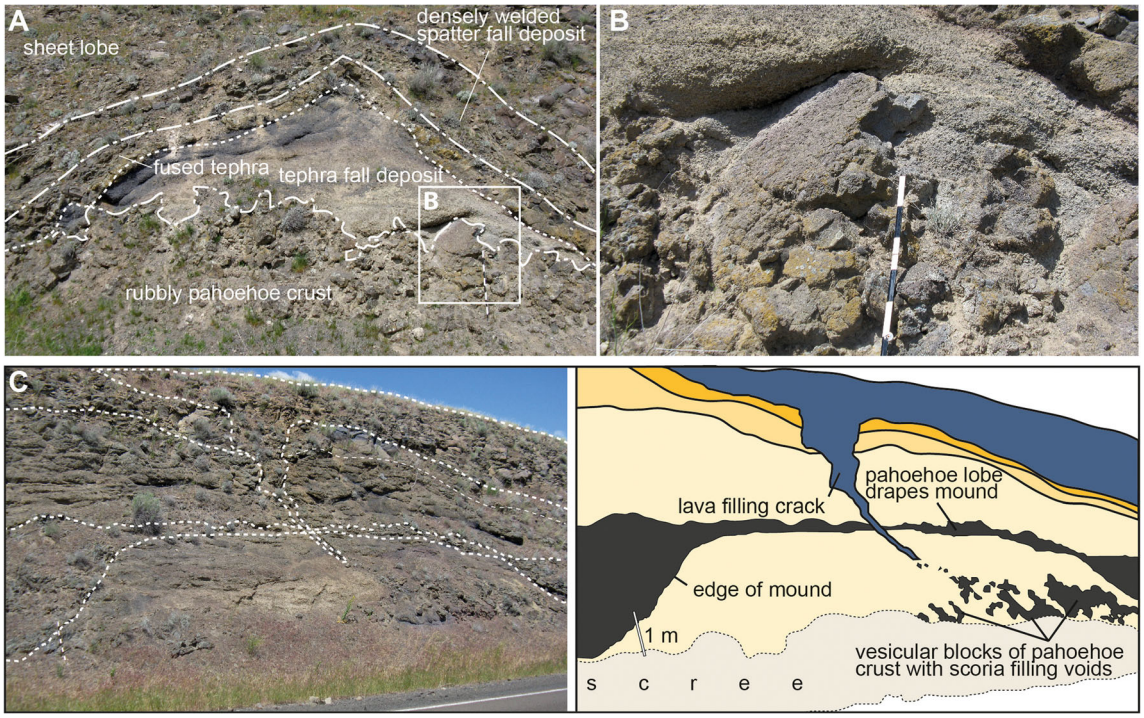

Fig. 3 **a** Typical mound of tephra in the Roza Member at Winona. Mound consists of a well-sorted, massive tephra fall deposit and overlies rubbly vesicular pāhoehoe crust in which lapilli fill the voids between slabs and blocks of crust. The mound is draped by welded fall deposits that have welded the clasts on the exterior of the mound. Metre rule for scale. See Fig. 2 for location. **b** Upturned slab of vesicular pāhoehoe crust at the base of a tephra mound. See Fig. 1 for location. Metre rule for scale. **c** Photograph and interpretive sketch of intercalated pāhoehoe lava and tephra within a mound at Winona (see Fig. 1 for location). Mound 1 overlies rubbly pāhoehoe, as in **b**, and is in turn buried by lava (*2*). *Lava 2* is overlain by a second tephra fall deposit, which has also been modified into a mound. This second mound has been draped by welded fall deposits and is buried beneath lava 3. A crack developed through the tephra deposits has been filled by lava 3. Lava 2 may have been fed by a breakout from a tumulus in lava 1. See Fig. 2 for key

lava flows are interbedded with tephra fall deposits (Fig. 2). Elsewhere, tephra that has percolated down into tumuli in underlying lobes has been thermally discoloured indicating that the underlying lava was still hot.

The upper mounds are draped by densely welded spatter deposits, and the exteriors of the mounds in contact with the spatter have been sintered to depths of 5–10 cm. The overlying deposits consist of ~65-cm-thick, finely crystalline, lava-like tuff with sparse spherical vesicles in its middle part. Sharply overlying this unit is ~40 cm of brown glassy welded tuff with ghost fiamme typically 1–1.5 cm long and <1–2 mm thick. This is sharply overlain by >12 m of dense, columnar jointed Roza lava. The lower two layers appear to have locally slumped on some mounds and occur twice or three times as a repeating sequence; elsewhere, small-scale disruption of the sequence is also consistent with slumping (Fig. 2). This indicates that the mounds are larger in 3D than they appear in 2D. One mound exhibits a subvertical downward-tapering crack that has been filled by Roza lava from the uppermost exposed dense lava (Fig. 3c, d).

Table 2 Physical characteristics of the tephra mounds in 2D man-made cuts through the Roza Member at Winona (Fig. 1)

d (m)	*h* (m)[a]	*w* (m)[a]	*Θ*	Morphology
–	4	20	24°	Double peaked
41	2	13	27°	Peaked
26	5	8	36°	Rounded
35	2.5	30	20°	Flat/rounded
35	4	16	24°	Flat topped
36	2.5	6	34°	Peaked
20	4	20	24°	Flat topped

d spacing centre to centre of mound from left to right, *h* height, *w* width, *Θ* mean slope angle

[a] Minimum values

Discrete mounds of variably oxidised agglutinate, spatter and moderately densely welded tephra outcrop on top of the uppermost Roza Member sheet lobe, at distances of <1 km from inferred fissure vents (Fig. 2). They are particularly common at the western end of the railway cut at Winona, where they outcrop across an area of <400 m^2 and are also well-exposed in Mason Draw (Table 1). Each mound is typically several metres high and has a cross-sectional area of several to tens-of-metres square. Most comprise massive to crudely bedded and densely to moderately welded spatter and scoria.

Clasts reach 25 cm in diameter. Bedding and spatter clast foliation dips are typically high (20–46°) and adjacent, but unconnected outcrops can exhibit strongly divergent dips and strikes. This crude foliation is commonly terminated by the edges of the mounds. The lower contacts with underlying sheet lobes are not exposed, but at Winona, the mounds outcrop at the same altitude as the underlying flow's vesicular upper crust, indicating that the upper surface of the sheet lobe had several metres of relief.

Two larger mounds of non-welded to densely welded pyroclastic rocks, interbedded with thin rubbly pāhoehoe lava, occur 2 km north of Winona. These are up to 15 m thick, 30 m wide and are draped by 2.5 m of non-welded to moderately welded scoria fall deposit.

Grande Ronde Member, Columbia River Basalt Group, USA

Tephra fall deposits occur within the 16 Ma Grande Ronde lavas (Barry et al. 2010) at Little Sheep Creek, Oregon (Table 1 and Fig. 4). They are interbedded with three lavas exposed along road cuts. The upper and lower lavas comprise thick (4–8 m) sheet lobes with rubbly, vesicular upper crusts that reach 5 m thick. These rubbly crusts are intruded by irregular, sub-vertical squeeze-ups of blocky-jointed dense lava core that have assimilated and agglutinated rubble onto their exteriors. Contacts with the rubble are glassy or gradational. The middle lava is overlain by a 10-m-thick scoria fall deposit exposed in a 150-m-long road cut (part of which is shown in Fig. 4). At this location, only the brecciated upper crust of the lava is exposed in the form of multiple sub-vertical protrusions of dense lava that are similar to those that pierce the rubbly crusts of the upper and lower lavas (Fig. 4). The tephra fall deposit is texturally similar to that described from the Roza Member and is massive to weakly bedded (Fig. 4). The tephra is strongly altered to palagonite, but the outlines of individual clasts and vesicles are still visible. The deposit is well-sorted, clast-supported and comprises scoria lapilli <2 cm in diameter. The squeeze-ups of lava are 0.1–3 m wide (Fig. 4) and extend upwards from an underlying sheet lobe that has a brecciated vesicular upper crust composed of variably vesicular blocks of lava, similar to that of the upper and lower sheet lavas. The cores of the intrusions are coherent, well-jointed, dense lava with scattered large gas vesicles up to 20 cm in diameter. The upward tapering intrusions are partially encased in a carapace of rubble (Fig. 4) and exhibit complex morphologies. Contacts between the rubble and the intrusions vary from sharp to gradational. A tephra fall deposit in contact with the squeeze-ups has been thermally oxidised to a depth of <1 m (Fig. 4). It is unclear if any protrusions reach the upper surface of the scoria fall deposit, which is overlain by lava. The uppermost few decimetres of the fall deposit have been oxidised by the overlying lava (Fig. 4).

Chinyero volcano, Tenerife, Canary Islands

The 1909 Chinyero eruption, Tenerife (Table 1 and Fig. 5) lasted for 10 days and produced a scoria cone, tephra fall deposits and a basaltic lava flow that covered ~2.7 km^2 (see Carracedo 2013). At least five vents were active during the lifetime of the volcano (see Carracedo 2013).

Field relationships indicate that the effusion of lava alternated and overlapped with the development of quasi-steady eruption plumes that dispersed lapilli and ash to the northwest. Significant portions of the scoria cone (blocks 8 m high) have been rafted up to 1 km from source, leaving a crescent-shaped pyroclastic construct standing 80 m high around the vent area (Fig. 5). An extensive a ā lava flow field extends southwards away from the vent.

The lava flow field is partially covered in tephra fall deposits derived from the eruption (Figs. 5 and 6). Stagnant parts of the lava flow remain covered in a smooth undisrupted tephra blanket that mantles the irregular surface of the lava flow. Lava that continued to flow from the vent after fallout ceased disrupted the overlying tephra blanket and generated a series of rafted tephra mounds along the margins of the flow (Fig. 6a, b, d). The mounds are up to 1.5 m high and have slopes of 20–36° (Table 3 and Fig. 6). Both isolated and connected mounds are present: isolated mounds are 2–10 m apart and 3–10 m wide. The lava flowed over more distal parts of the same tephra blanket that lay on top of it, resulting in a repetition of the fall deposit (Fig. 6c): the lower layer is finer-grained than the rafted layer which was carried several hundred metres on top of the lava. Parts of the lava flow field that post-date fallout and do not have disrupted mounds on top of them are devoid of tephra cover (Fig. 6d).

Hekla volcano, Iceland

The 1991 eruption of Hekla, Iceland began with a ~1-h-long explosive Subplinian (initial) phase that produced a ≥11.5-km-high eruption column and a north-northeast dispersed plume with significant tephra fall up to 370 km from the volcano (Gudmundsson et al. 1992). This was followed by stepwise unzipping of the Hekla fissure to the southwest of the summit crater as well as to the base of the eastern flank, forming a 5-km-long fountaining fissure across the volcano (Fig. 7). This phase of the eruption was characterised by simultaneous explosive and lava fountain activity, producing tephra-rich columns, 300–500-m-high lava fountains and fountain-fed lava flows that cascaded down the western, southern and eastern slopes of the volcano, reaching lengths of 4–5.5 km in <6 h. Shortly thereafter, new lava fountains emerged from radial northern and southern fissures (Fig. 7). During the ~1-h-long Subplinian summit phase, the magma

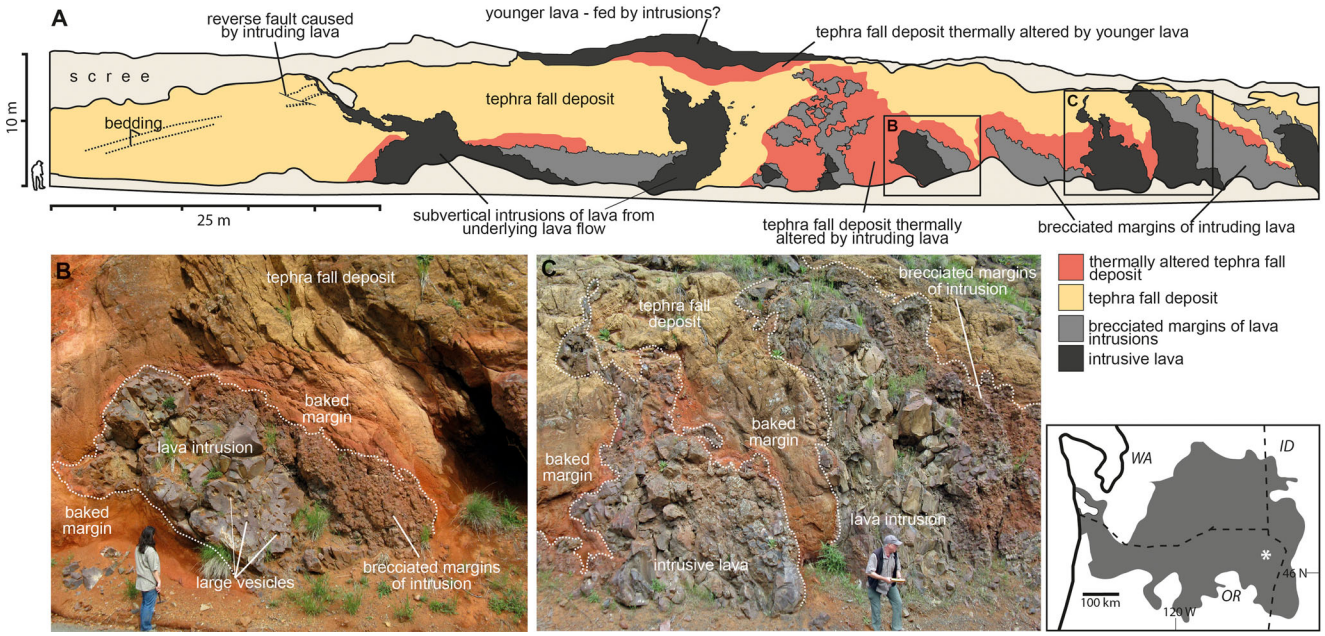

Fig. 4 Lava intrusions in a tephra fall deposit fed by breakouts from an underlying inflating lava flow of the Grande Ronde lavas, CRBG. **a** Sketch of roadcut showing irregular intrusions cutting through a thick tephra fall deposit. Margins of the intrusions are locally brecciated and have thermally altered the host deposit. Intrusions strike nearly parallel to the roadcut. Vent location for the tephra deposits is not known. **b** Stubby intrusion showing dense interior with large gas cavities. Note thermal alteration (*orange oxidation*) of host rock. **c** Multiple intrusions with brecciated margins (*right*) and thermal alteration. Intrusion on *left* appears to taper upwards. Inset map shows location (*asterisk*; see also Table 1); extent of CRBG lavas shown in *grey shade*

discharge was just over 2,000 m^3/s, whereas during the fissure forming phase, the discharge dropped abruptly to <20 m^3/s in the course of 3 days (Gudmundsson et al. 1992). This decline in magma discharge coincided with an eastward shift in the activity as well as gradual decrease in eruption intensity and progressive localization of the active vents towards the

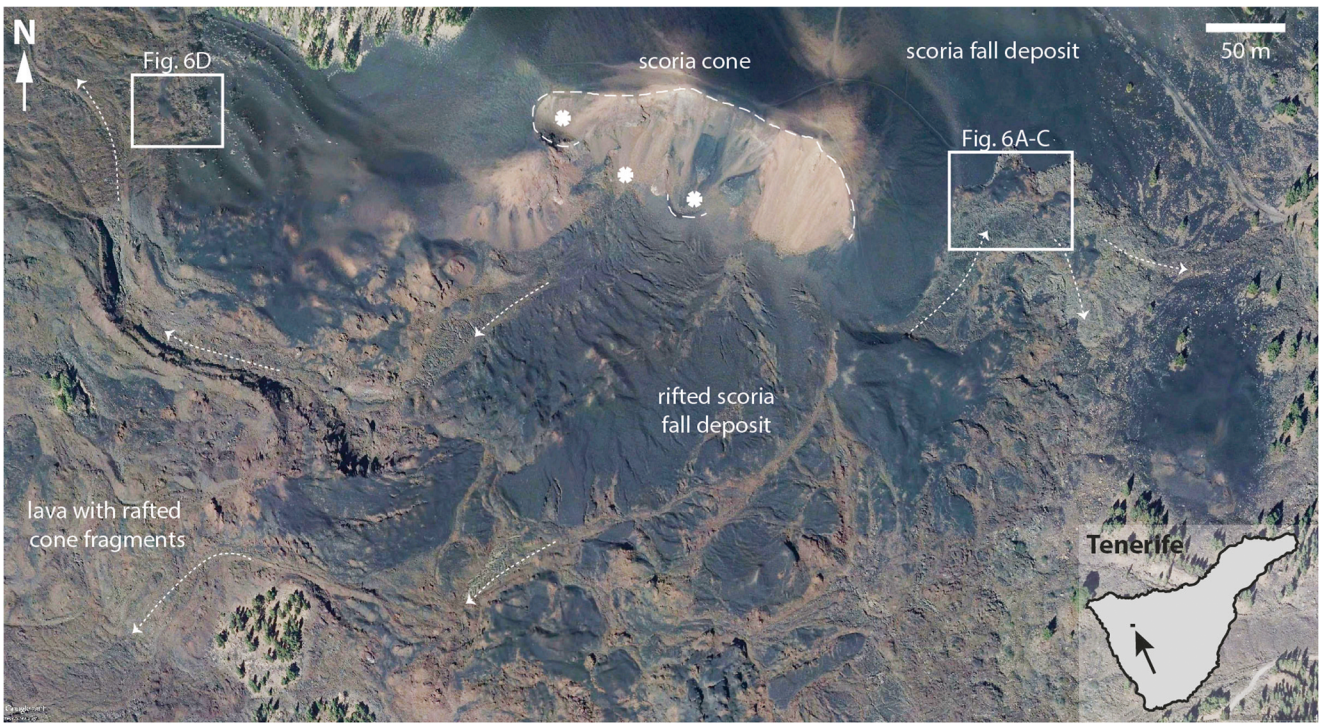

Fig. 5 Interpreted satellite image of the 1909 Chinyero scoria cone and erupted products, Tenerife. Scoria fall deposit south of the scoria cone has rifted apart on top of lava flows. *Arrows* show main lava pathways. Image from Google™ Earth Pro

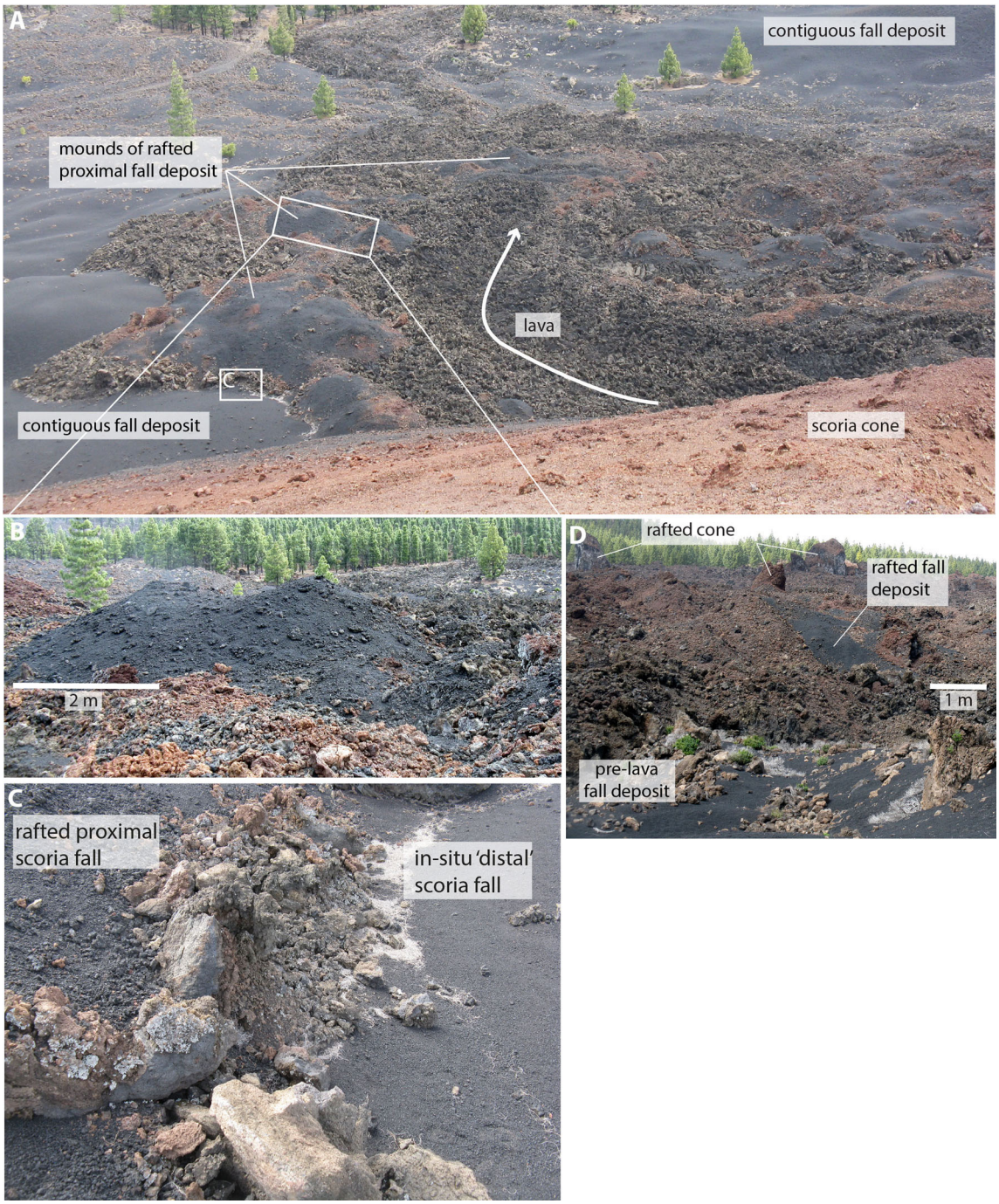

Fig. 6 Dissected tephra fall deposits of the 1909 eruption of Chinyero, Tenerife. **a** View east from the Chinyero scoria cone showing how the proximal tephra sheet has been transported and disrupted into mounds on top of a rubbly lava flow. Distal parts of the tephra sheet have been overridden by the lava. **b** Detail of disrupted tephra mounds. Note similarity to those in Figs. 2 and 3. **c** Tephra blanket on *right of photo* is inferred to be the same age as that on the *left*, which has been transported from a more proximal position on top of lava. **d** Remnants of tephra fall deposit on main lava flow from the Chinyero eruption situated west of the main cone (see Fig. 5 for location). Note large rafted blocks of scoria cone in distance

easternmost part of the Hekla fissure. By the third day of the eruption, the activity was characterised by lava fountaining on a short (<500 m long) fissure segment at the site of the East Cone (Fig. 7). Two days later, the activity was characterised by a single gas jet carrying sporadic bombs to heights of several hundred metres with only minor amounts of ash. Coarse ejecta gradually piled up around the vent to form the 80-m-high and ~250-m-wide East Cone. At the same time, lava was discharged at rates of 1–12 m^3/s, feeding the 'normal' lava flows through several vents below the East Cone.

Table 3 Physical characteristics of tephra mounds on the north portion the Chinyero lava flow, Tenerife

h (m)[a]	*w* (m)[a]	*Θ*	Morphology
2	5	20°	Peaked
2	8	22°	Double peaked
1	3	36°	Peaked
2.5	6	32°	Peaked
2.5	25	32°	Hummocky
<1	3	36°	Peaked
<1	4.5	21°	Flat topped

h height, *w* width, *Θ* mean slope angle

[a] Minimum values

During the first 3–4 days, the fissure segment, now represented by the East Cone, featured intense lava fountaining that blanketed the immediate surroundings (up to 1–1.5 km from the vents) with fallout, which on the surface was represented by a continuous blanket of tephra. The surface slope in this area was 5–10°.

Shortly thereafter, arcuate tension cracks opened up in this tephra blanket to the north and east over a rectangular area of 0.15 km^2 (Fig. 8a). The cracks are oriented transverse to the dip of the slope, 5 m wide and up to 5–9 m deep which at the time of the eruption extended down through 3–6 m of lapilli tephra fall deposit and up to 3 m of incipiently to intensely welded spatter deposit into an incandescent horizon that formed the basal clastogenic lava that was still creeping downslope at the time of observation by one of the authors (Thordarson) (Fig. 8b–d). As the incandescent clastogenic part crept downslope, the overlying and then unconsolidated welded spatter units and unconsolidated lapilli tephra units underwent extension and broke up into series of lenticular coherent blocks, each up to several metres wide and several hundred metres long (Fig. 8). During downslope creep, some tephra blocks underwent small degrees of rotation, which resulted in their upper surfaces dipping upslope by <15°, and therefore these may in some instances resemble listric faults. Small grabens developed with vertical displacements of <1 m. The area that underwent downslope creep was bound by a discontinuous head scarp (Fig. 8).

The overlying scoria fall deposit had a significant coherence through the interlocking of angular and spinose tephra. This allowed the non-welded deposit to maintain steep, vertical and slightly overhanging faces during fissure and tension crack development and lateral spread. However, small talus fans of scoria within the cracks

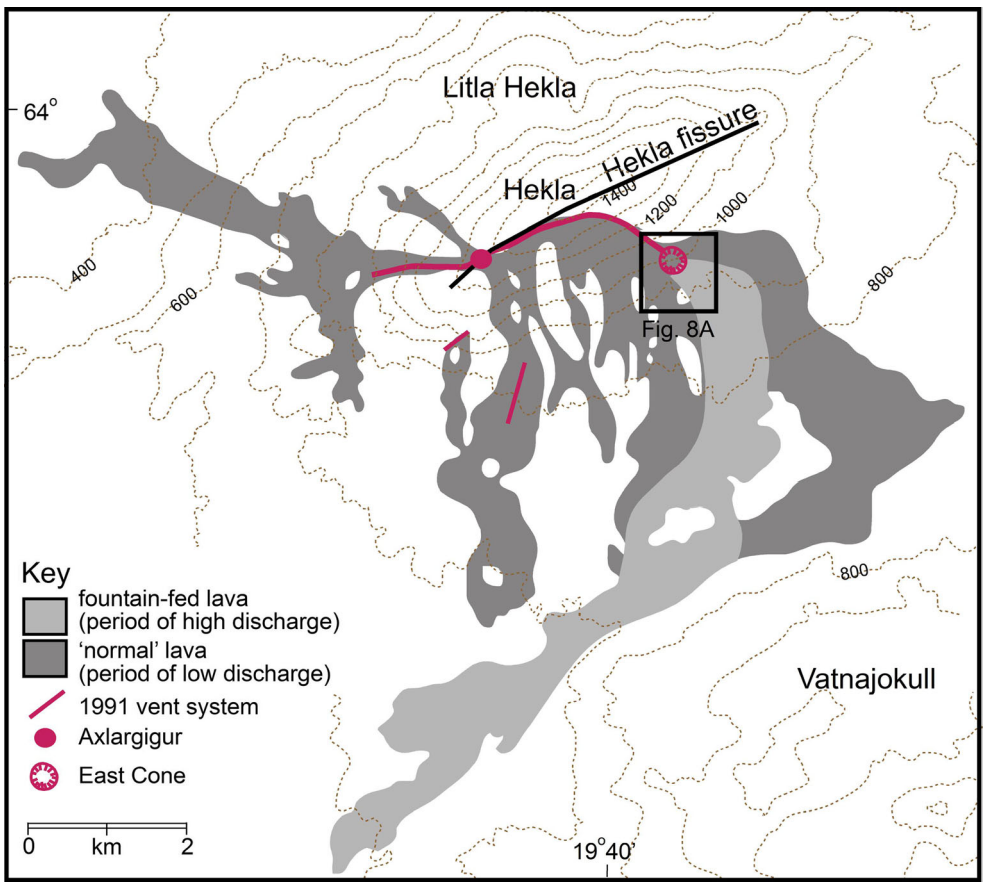

Fig. 7 Geological sketch map of the products of the 1991 eruption of Hekla, Iceland. Modified from Gudmundsson et al. (1992)

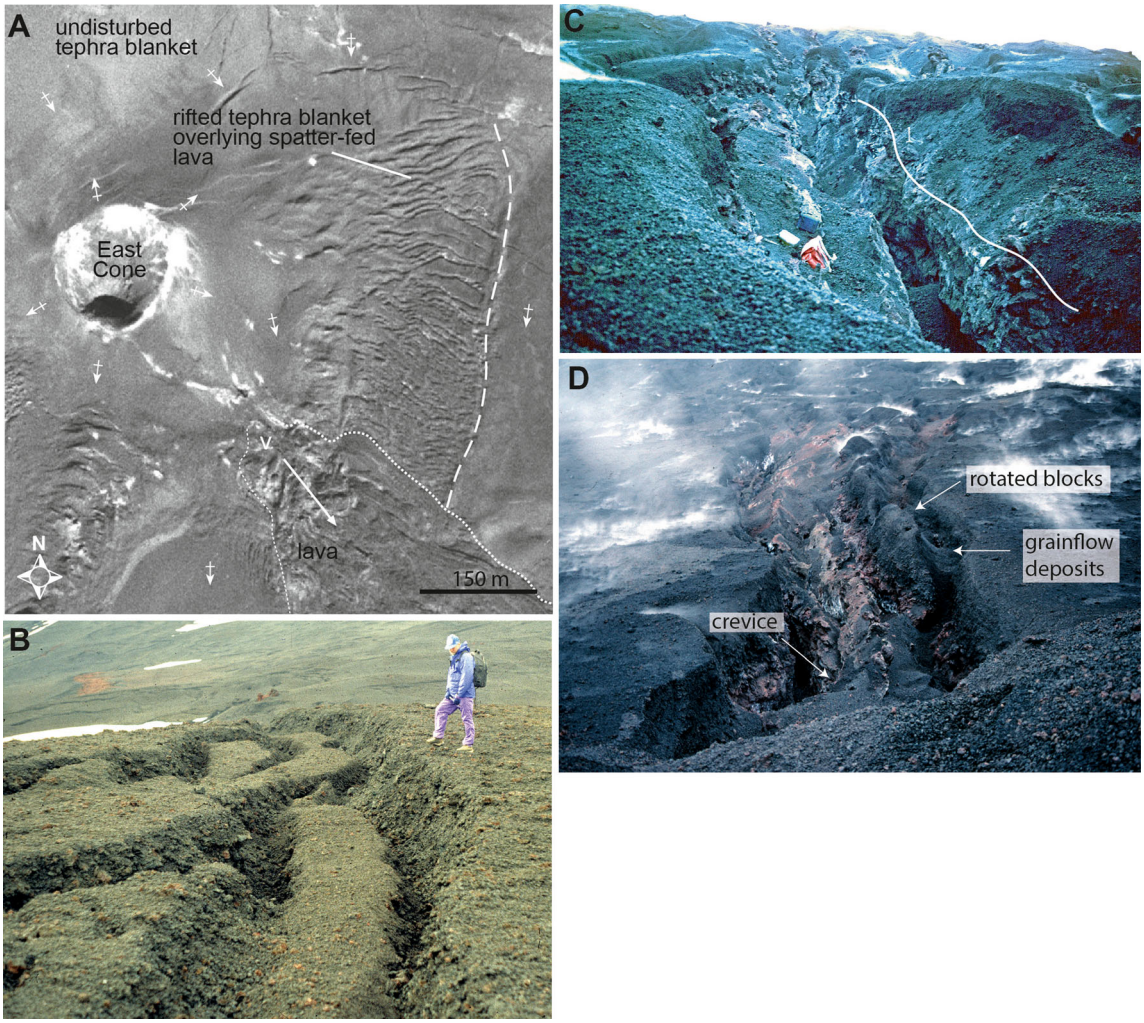

Fig. 8 Disrupted tephra fall deposits of the 1991 eruption of Hekla, Iceland. **a** Aerial photograph of the East Cone and disrupted fall deposit. *Arrows* indicate downhill slope direction. **b** Extensional fissures in the disrupted tephra fall deposit. **c** Deep fissures exposing coarse-grained spatter. Bag for scale. Line marks base of non-welded tephra. **d** Rotated block within extensional fissure

(Fig. 8b–d) are built up by collapse and grain flow during or shortly after rifting. The initially vertical sides of the blocks became subdued over time as material collapsed into the crevices, in many cases almost completely filling the cracks (Fig. 8). Over time, the jagged topography became subdued into a series of low convex ridges aligned sub-parallel to the strike of the slope.

Examples of similar formations, comprised of a series of elongate tephra mounds and underlain by clastogenic lava, although with much less jagged topography, are present in an historic lava flow that crops out on the NE slopes of Hekla between the northernmost lava branches of the 1980 and 1991 events (Fig. 7). By the same token, similar tephra mounds crop out in the near-vent region of the 1783–1785 Laki eruption, namely in the south side of the Hnúta vent segment and within the lava in Varmárdalur straight west of the northwest end of Galti (Table 1).

Interpretation and discussion

Formation of the tephra mounds

The examples described above illustrate how tephra fall deposits can become disrupted and dissected during basaltic eruptions. The examples from the CRBG provide 2D cross sections through tephra sheets, whereas the examples from Tenerife and Iceland allow the 3D morphology of the deposits to be examined.

The tephra deposits of the Roza Member at Winona are inferred to have been deposited at distances of >800 m from a vent that is exposed in the railway cut (Fig. 2; Brown et al. 2014). Truncation of sub-horizontal bedding by the edges of some mounds demonstrates that the tephra deposits originally mantled the substrate as continuous sheets (Fig. 2). There are several possible explanations for how these sheet-form fall deposits could have become dissected into partially

connected and unconnected mounds. Swanson et al. (1975) envisaged that the mounds formed due to bulldozing by advancing lava flows, but this should result in chaotic mounds with severely disrupted bedding. Erosion of the fall deposit by surface water is discounted due to the absence of evidence for aqueous reworking (e.g. scours, rills or gullies). The high porosity and permeability of the coarse-grained fall deposits, combined with the low palaeoslope angles, would have inhibited surface runoff.

Instead, we favour an interpretation whereby the tephra sheets were disrupted into mounds by an underlying lava flow, which was still moving (Fig. 9), through some combination of lateral (flow) and vertical (differential inflation) movement. This interpretation is backed up by the similarities in morphologies and dimensions between the Roza tephra mounds and those on top of the Chinyero lavas, which clearly rafted on top of a lava flow (see Figs. 2 and 6; e.g. Holm 1987; Valentine et al. 2006; Riggs and Duffield 2008). The underlying lavas in both cases are characterised by rubbly crusts with metre-scale relief. In the Roza Member, tephra that has percolated down into void spaces in the rubbly tops of the lava and has been thermally oxidised by the lava confirms that fallout occurred on top of active lava flows. We infer that extension of the tephra sheet enabled grain flow and collapse of scoria lapilli away from the separated parts of the fall deposits (Fig. 9). The irregular, spiny shapes and interlocking nature of the lapilli meant that free surfaces would maintain steep slope angles on the exteriors of some mounds for a short period (months to years). Mounds with convex morphologies and shallower slope angles may have been modified by the gravitational remobilisation of loose scoria into the depressions (e.g. by grain flow, collapse): this may also indicate that a significant period (months to years) passed before they were covered by younger deposits (the Roza eruption is considered to have lasted years, Thordarson and Self 1998). The well-sorted nature of the tephra and the short distance (from the scarp of the fracture to the bottom of the fracture) over which remobilisation operated means that it would be difficult to distinguish remobilised deposits from in situ deposits (except where bedding is present).

The presence of interbedded lava flows and tephra fall deposits in the Roza Member indicates that effusion of lava and fallout from eruption columns was synchronous or alternated during successive phases of the eruption. Some thin vesicular lava flows intercalated within fall deposits may have been fed by breakouts of lava from subjacent tumuli during inflation (e.g. Fig. 2). Breakouts could have intruded up through the overlying tephra fall deposit and then started to flow across the fall deposit's upper surface as lobes of gas-rich pāhoehoe lava (Fig. 9). Field relationships indicate that they ponded within depressions between mounds (Fig. 2). The intrusions into the scoria fall deposit of the Grande Ronde lavas (Fig. 4) are interpreted in a similar manner. Tephra fell out on top of an active lava flow. As the underlying lava flow inflated, tumuli developed and breakouts of viscous degassed lava were injected upwards through the tephra fall deposit. The margins of the intrusions chilled and brecciated against the overlying enclosing fall deposit and in doing so thermally oxidised it (Fig. 4). As inferred for the Roza Member, some of these intrusions may have reached the surface of the tephra fall deposit and then flowed across the surface of the lava flow as pāhoehoe lobes, but it currently cannot be proven from the field relationships.

Disruption of the tephra sheet at Hekla was achieved in a manner similar to that outlined above. Here, though, viscous flow occurred in a layer of clastogenic lava beneath coherent non-welded tephra fall and spatter deposits (Fig. 8). As this clastogenic lava flowed downslope, the overlying fall deposit behaved as a brittle coherent mass under extension (Fig. 8). We speculate that the overlying tephra deposits acted to

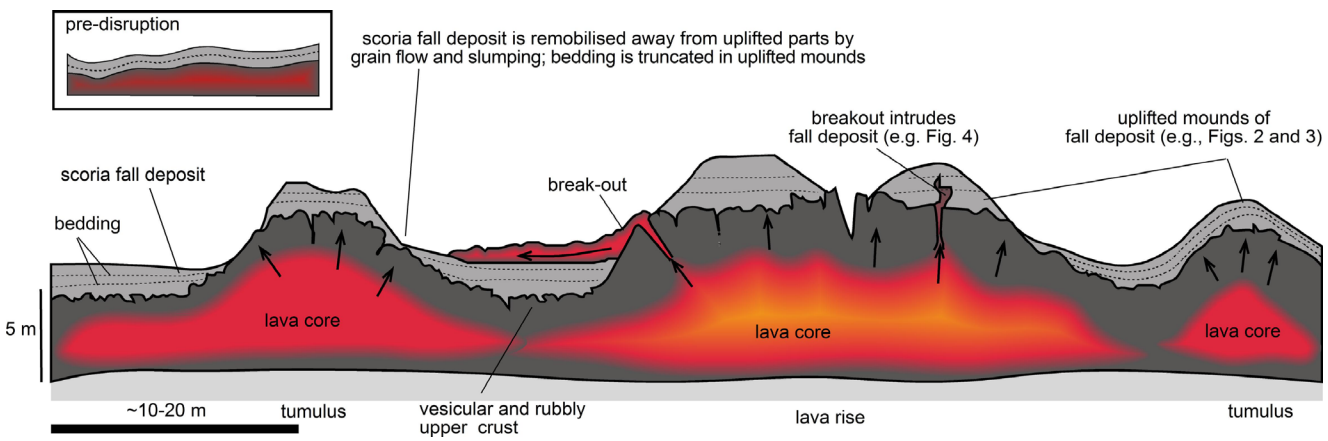

Fig. 9 Cartoon illustrating the disruption of a sheet-form tephra fall deposit into partially connected mounds by the inflation and lateral spread of a subjacent lava flow. Breakouts may flow across the surface of tephra deposits or may intrude into overlying fall deposits. *Inset* shows tephra deposit prior to disruption

insulate the clastogenic lava, but that once spreading occurred, heat loss through open cracks and fissures may have led to higher rates of cooling and may have acted to slow and eventually halt viscous flow. Similar tension cracks within scoria fall deposits were observed on the shoulders of the Pu u Ō ō cone, Kīlauea volcano, Hawai i (Heliker et al. 2003) and on many of the cones formed during the 1783–1785 eruption of Laki. At Kīlauea volcano, these cracks penetrated subjacent incandescent material that was inferred to have been creeping downslope (Heliker et al. 2003).

The spatter mounds on the tops of the Roza sheet lobes form discrete outcrops of variably dipping pyroclastic material that are texturally and compositionally similar to the pyroclastic deposits that form proximal vent constructs in the Roza Member (Brown et al. 2014). We infer that they are the remnants of proximal constructs, such as spatter ramparts that have been rafted from the vent in lava channels (see also Chinyero volcano, Fig. 6d). This differs from the other outcrops described here (e.g. in the Roza Member at Winona and at Hekla), in that the transport distance is much greater, and the other outcrops record disruption of tephra sheets, rather than proximal edifices. Rafted segments of pyroclastic edifices, reaching up to several hundred metres wide, have been documented at other volcanoes (e.g. Holm 1987; Valentine et al. 2006; Riggs and Duffield 2008) and are generated when lava breaches or undermines scoria cones or spatter ramparts. Because the pyroclastic material is of lower bulk density (e.g. average bulk density of 1,700 kg/m^3 for the Roza Member, Brown et al. 2014) than the lava, it can be carried for several kilometres as flotsam in open channels (Holm 1987; Riggs and Duffield 2008). The occurrence of rafted spatter ramparts over areas of ~0.5 km^2 in the Roza Member is consistent with major breaches of proximal constructs by lava.

Implications for reconstructing stratigraphic relationship and tephra fall isopach maps for basaltic eruptions

Tephra fall deposits contain information (e.g. thickness, maximum clast size) that can be used to probe and quantify the dynamics of explosive volcanic eruptions (e.g. Carey and Sparks 1986; Wilson and Walker 1987; Pyle 1989; Parfitt and Wilson 1999; Houghton et al. 2006). This is best achieved where deposits are accessible, well-preserved, well-exposed and unaffected by erosion or weathering, and it becomes more difficult the more eroded or more poorly exposed a deposit is. Proximal deposits are important in the construction of total grain size distributions of fall deposits, which can be used to infer fragmentation and eruption style and help understand plume dynamics (Bonadonna and Houghton 2005). Our observations from the USA, Tenerife and Iceland illustrate the ways in which pyroclastic deposits can become disrupted in proximal regions during basaltic eruptions, resulting in complex stratigraphical relationships between lavas and pyroclastic deposits. These mechanisms include lateral and vertical displacement caused by movement of underlying lavas, rafting of strata from proximal edifices atop lava flows and downslope creep and lateral spread initiated by rheomorphic flow of clastogenic lava. Some of these outlined processes have resulted in the repetition of fall layers (e.g. Fig. 2). Whilst these processes can be observable in the products of young eruptions (Fig. 6), such relationships become difficult to recognise in poorly exposed deposits or in those in the geologic record. This can be compounded because fall deposits and lavas from basaltic eruptions can show little textural, physical or chemical variation. This results in an absence of distinct marker horizons with which to correlate similar-looking sequences between outcrops.

The relationships outlined here indicate that tephra fallout either alternated or was synchronous with the emplacement of lava flow fields. These situations could arise if the lava flows are fed by vigorous fountains (>0.5 km in height) or if pyroclastic material and lava are emitted from separate vents along a fissure. During synchronous lava effusion and fallout, the bases and the tops of tephra deposits may well be diachronous where they are in contact with advancing lava flows (the tops and bases of lava flow fields are always diachronous) (Fig. 10). As an example, pāhoehoe flow fields advance by successive metre to sub-metre-sized breakouts of lava at rates of 0.01–0.7 km/h (e.g. Thordarson and Self 1993; Hon et al. 1994), whilst fallout during basaltic eruptions can last for many hours to days (e.g. Rowland et al. 2009). Advancing lava will transgress depochrons (cryptic lines joining particles deposited at the same time; after Branney and Kokelaar 2002) within the accumulating fall deposit. This means that that pyroclasts lying on top of the lava flow field in proximal locations correlate with pyroclasts beneath that same flow field in more distal locations (Fig. 10). Additionally, given that the pathways of advancing lava are determined by the substrate topography and by the flow field's internal lava transport system, the paving of ground by lava may be highly irregular through time and space. This is achieved by lobes that split, converge, accelerate and decelerate non-uniformly and can result in the formation of kipukas and lava rise pits (e.g. Walker 1991). Complex temporal and spatial relationships between flow fields and any coeval tephra fall deposits may remain cryptic in the geological record. In modern deposits, such relationships might not be apparent due to partial burial of fall deposits by later erupted lavas. Breakouts from tumuli could feed small secondary lava flows that spread across the upper surface of the fall deposit rather than the upper surface of the lava (Fig. 9). Whilst this has not been proven to have occurred in the CRBG examples, the field relationships seen there (Figs. 2 and 4) and observations of breakouts from modern pāhoehoe lava flows demonstrate that this is possible. This would act to further complicate outcrop-scale stratigraphic relationships between fall deposits and lavas in proximal environments.

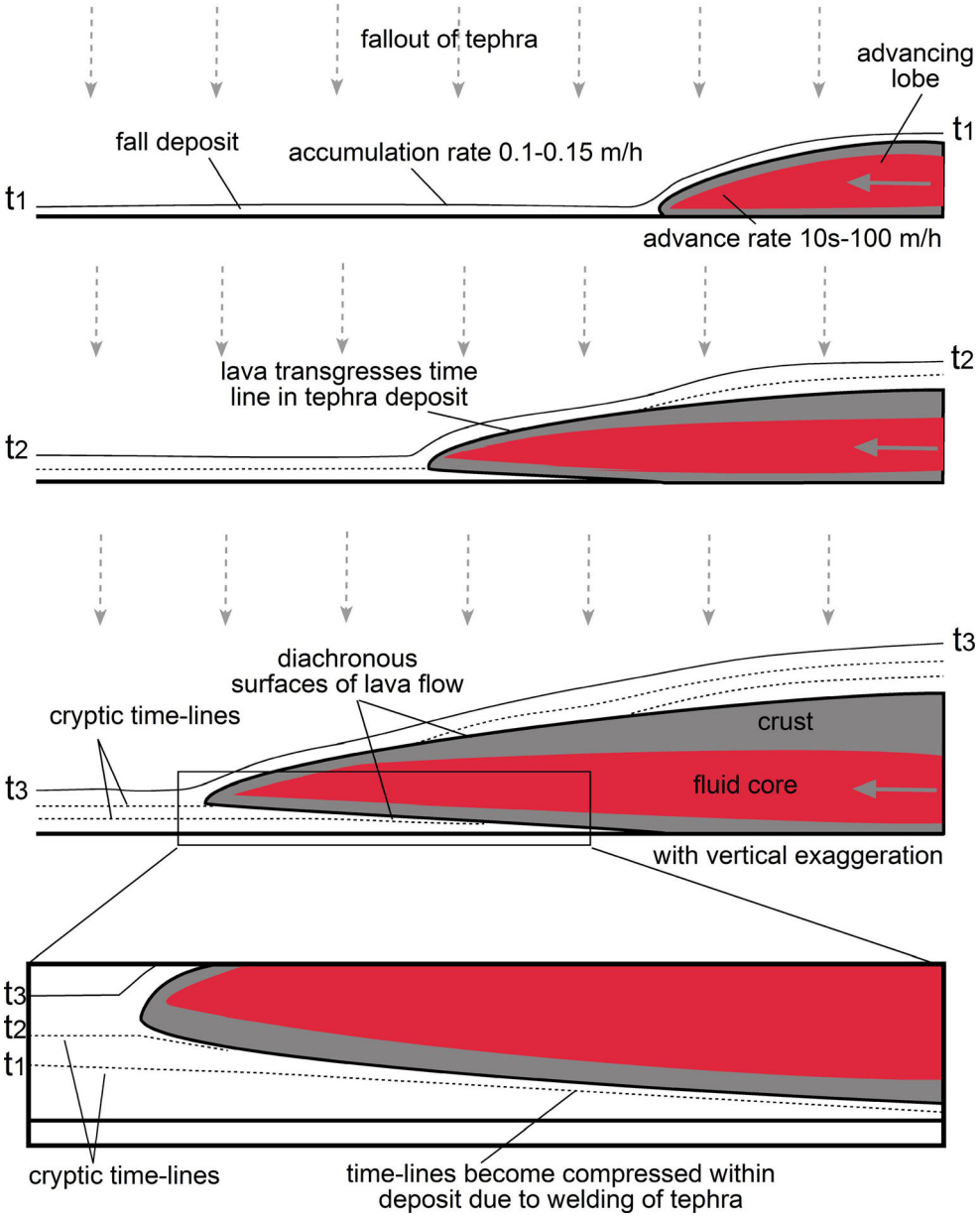

Fig. 10 Cartoon to illustrate the hypothetical diachronous relationships between a synchronously emplaced lava flow and a tephra fall deposit in vent-proximal regions. Relationships are likely to remain cryptic due to the common physical, textural and chemical homogeneity of basaltic fall deposits and to complex lava pathways

The eruptions of Chinyero, Tenerife only lasted for 10 days (Carracedo 2013), whilst Hekla continued for <8 weeks (Gudmundsson et al. 1992). The potential for the disruption of fall deposits increases the longer an eruption lasts. For flood basalt eruptions, thought to last years to tens-of-years (Thordarson and Self 1998; Self et al. 2006), disruption of tephra deposits due to interaction with lavas is almost inevitable. Lava flows fed by effusion from one vent can inundate large areas prior to the opening of another vent along the fissure, and actively inflating sheet lobes can receive fallout onto their deforming upper crusts. Given that the fissure system that fed the Roza Member was >180 km long and was host to numerous vents (Brown et al. 2014), the sorts of processes outlined here should be expected.

Conclusions

Proximal outcrops through flood basalt flow fields and tephra deposits in the northwest USA, and tephra deposits from modern and historic basaltic eruptions on Iceland and Tenerife, illustrate how once-continuous tephra fall deposits can become disrupted through movement of underlying lavas emitted during the same eruption. The inferred range of lateral displacement in these examples varies from metres to 100 s metres, and the resultant structures vary from extended (rifted) sheets through to isolated mounds and ridges. In the Roza Member, CRBG and at Chinyero, Tenerife, proximal tephra sheets have been disrupted on top of pāhoehoe sheet lobes that were inflating during and following fall out. Lateral and

vertical movement of the upper crust of the pāhoehoe flow resulted in the formation of mounds of tephra. In the Grande Ronde Member, CRBG, squeeze-ups from active lava flows have intruded into overlying tephra fall deposits from the same eruption. Leakage of lava out of the upper crust of inflating pāhoehoe lava flows up through overlying tephra deposits can result in complicated stratigraphic relationships. At Hekla, Iceland, downslope creep in a clastogenic lava led to the rifting apart of overlying non-welded tephra fall deposit to form a series of steep-sided ridges and fissures. We recommend that the sorts of structures and field relationships presented here for proximal environments for basaltic eruptions should be sought out and avoided when collecting data for isopach or isopleth maps. Disruption of tephra sheets can result in modification of the original deposit thickness, and to allochthonous outcrops of tephra, to diachronous and complicated relationships between coeval tephra fall deposits and lavas. These complexities may remain cryptic in the field due to the common textural, physical and geochemical similarity of lavas and of tephra deposits emplaced during any one basaltic eruption.

Acknowledgments Research in the CRBG was funded by a Natural Environment Research Council Standard Grant (NE/E019021/1) awarded to S. Self. T. Thordarson was partly funded by NASA and the University of Hawai i. We thank C. Parcheta and S. Rowland for positive and constructive reviews and M. Patrick for editorial assistance and advice.

References

Barry TL, Self S, Kelley SP, Reidel S, Hooper P, Widdowson M (2010) New $^{40}Ar/^{39}Ar$ dating of the Grande Ronde lavas, Columbia River basalts, USA: implications for duration of flood basalt eruption episodes. Lithos 118:213–222

Bonadonna C, Houghton BF (2005) Total grain-size distribution and volume of tephra fall deposits. Bull Volcanol 67:441–456

Branney MJ, Kokelaar P (2002) Pyroclastic density currents and the sedimentation of ignimbrites. Geol Soc Lond Mem 27:1–152

Brown RJ, Blake S, Thordarson T, Self S (2014) Eruption processes, pyroclastic deposits and volcanic edifices of flood basalt fissure eruptions (The Roza Member, Columbia River Basalt Province, US). Geol Soc Am Bull 126:875–891

Carey S, Sparks RSJ (1986) Quantitative models of the fallout and dispersal of tephra from volcanic eruption columns. Bull Volcanol 48:109–125

Carracedo JC (2013) The last 2 ky of eruptive activity of the teide volcanic complex: features and trends. In: Troll VR, Carrecedo JC (eds) Teide volcano. Springer, Berlin, pp 129–153

Carracedo JC, Rodriguez Badiola E, Solera V (1992) The 1730–1736 eruption of Lanzarote, Canary Islands: a long, high-magnitude basaltic fissure eruption. J Volcanol Geotherm Res 53:239–250

Duraiswami RA, Bondre NR, Managave S (2008) Morphology of rubbly pāhoehoe (simple) flows from the Deccan volcanic province: implications for style of emplacement. J Volcanol Geotherm Res 177:822–836

Fedotov SA, Chirkov AM, Gusev NA, Kovalev GN, Slezin Yu B (1980) The large fissure eruption in the region of Plosky Tolbachik volcano in Kamchatka, 1975–1976. Bull Volcanol 43:47–60

Gudmundsson A, Oskarsson N, Gronvold K, Saemundsson K, Sigurdsson O, Stefansson R, Gislason SR, Einarsson P, Brandsdottir B, Larsen G, Johannesson H, Thordarson T (1992) The 1991 eruption of Hekla, Iceland. Bull Volcanol 54:238–246

Guilbaud M-N, Self S, Thordarson T, Blake S (2005) Morphology, surface structures, and emplacement of lavas produced by Laki, A.D. 1783-1784. Geol Soc Am Spec Pap 396:81–102

Heliker C, Kauahikaua J, Sherrod DR, Lisowski M, Cervelli P (2003) The rise and fall of Pu u Ō ō Cone, 1983-2002. In: Heliker C, Swanson DA, Takahashi TJ (eds) Pu u ʻŌ ō-Kūpainaha eruption, Kīlaeua volcano, Hawai'i: the first 20 years. USGS Prof Paper 1676:29–52

Holm RF (1987) Significance of agglutinate mounds on lava flows associated with monogenetic cones: an example at Sunset Crater, northern Arizona. Geol Soc Am Bull 99:319–324

Hon K, Kauahikaua J, Denlinger R, Mackay K (1994) Emplacement and inflation of pāhoehoe sheet flows: observations and measurements of active lava flows on Kīlauea volcano, Hawai'i. Geol Soc Am Bull 106:351–370

Houghton BF, Bonadonna C, Gregg CE, Johnston DM, Cousins WJ, Cole JW, Del Carlo P (2006) Proximal tephra hazards: recent eruption studies applied to volcanic risk in the Auckland volcanic field, New Zealand. J Volcanol Geotherm Res 155:138–149

Keszthelyi L, Thordarson T, McEwen A, Haack A, Guilbaud MN, Self S, Rossi MJ (2004) Icelandic analogs to Martian flood lavas. Geochem Geophys Geosyst 5:Q11014. doi:10.1029/2004GC000758

Lopez T, Thomas HE, Prata AJ, Amigo A, Fee D, Moriano D (2014) Volcanic plume characteristics determined using an infrared imaging camera. J Volcanol Geotherm Res 300:148–166

Martin BS (1989) The Roza Member, Columbia River Basalt Group: chemical stratigraphy and flow distribution. In: Reidel SP, Hooper PR (eds) Volcanism and tectonism in the Columbia River flood basalt province. Geol Soc Am Spec Paper 239:85–104

Parcheta CE, Houghton BF, Swanson DA (2012) Hawaiian fissure fountains 1: decoding deposits—episode 1 of the 1969–1974 Mauna Ulu eruption. Bull Volcanol 74:1729–1743

Parfitt EA, Wilson L (1999) A Plinian treatment of fallout from Hawaiian lava fountains. J Volcanol Geotherm Res 88:67–75

Passmore E, Maclennan J, Fitton G, Thordarson T (2012) Mush disaggregation in basaltic magma chambers: evidence from the AD 1783 Laki eruption. J Pet 53:2593–2623

Pioli L, Azzopardi BJ, Cashman KV (2009) Controls on the explosivity of scoria cone eruptions: magma segregation at conduit junctions. J Volcanol Geotherm Res 186:407–415. doi:10.1016/j.jvolgeores.2009.07.014

Pyle DM (1989) The thickness volume and grainsize of tephra fall deposits. Bull Volcanol 51:1–15

Richter DH, Eaton JP, Murata KJ, Ault WU, Krivoy HL (1970) Chronological narrative of the 1959–60 eruption of Kīlauea volcano, Hawai'i. In: The 1959–60 eruption of Kīlauea volcano, Hawai'i. US Geol Surv Prof Pap 537-E:E1–E73

Riggs NR, Duffield WA (2008) Record of complex scoria cone eruptive activity at Red Mountain, Arizona, USA, and implications for monogenetic mafic volcanoes. J Volcanol Geotherm Res 178:763–776

Rowland SK, Jurado-Chichay Z, Ernst G, Walker GPL (2009) Pyroclastic deposits and lava flows from the 1759–1774 eruption of El Jorullo, Mexico: aspects of 'violent Strombolian' activity and comparison with Parícutin. In: Thordarson T, Self S, Larsen G, Rowland SK, Hoskuldsson A (eds) Studies in volcanology: the legacy of George Walker. Special Publications of IAVCEI, Geol Soc London 2:105–128

Self S, Widdowson M, Thordarson T, Jay AE (2006) Volatile fluxes during flood basalt eruptions and potential effects on the global environment: a Deccan perspective. Earth Planet Sci Lett 248:518–532

Sigmarsson O, Condomines M, Gronvold K, Thordarson T (1991) Extreme magma homogeneity in the Laki 1783-84 Lakagigar eruption: origin of a large volume of evolved basalt in Iceland. Geophys Res Lett 18:2229–2232

Swanson DA, Wright TL, Helz RT (1975) Linear vent systems and estimated rates of magma production and eruption for the Yakima basalt of the Columbia plateau. Am J Sci 275:877–905

Thordarson T, Self S (1993) The Laki (Skaftár Fires) and Grímsvötn eruptions in 1783–1785. Bull Volcanol 55:233–263

Thordarson T, Self S (1996) Sulfur, chlorine and fluorine degassing and atmospheric loading by the Roza eruption, Columbia River Basalt Group, Washington, USA. J Volcanol Geotherm Res 74:49–73

Thordarson T, Self S (1998) The Roza Member, Columbia River Basalt Group: a gigantic pāhoehoe lava flow field formed by endogenous processes. J Geophys Res 103:27,411–27,445

Valentine GA, Perry FV, Krier D, Keating GN, Kelley RE, Coghill AH (2006) Small-volume basaltic volcanoes: eruptive products and processes, and post-eruptive geomorphic evolution in Crater Flat (Pleistocene), southern Nevada. Geol Soc Am Bull 118:1313–1330

Vye-Brown C, Gannoun A, Barry TL, Self S, Burton KW (2013) Osmium isotope variations accompanying the eruption of a single lava flow field in the Columbia River Flood Basalt Province. Earth Planet Sci Lett 368:183–194

Walker GPL (1991) Structure, and origin by injection of lava under surface crust, of tumuli, “lava rises”, “lava-rise pits”, and “lava-inflation clefts” in Hawaii. Bull Volcanol 53:546–558

Wilson L, Walker GPL (1987) Explosive volcanic eruptions—VI. Ejecta dispersal in Plinian eruptions: the control of eruption conditions and atmospheric properties. Geophys J Int 89:657–679